

**2444-18**

**College on Soil Physics – 30th Anniversary (1983–2013)**

***25 February – 1 March, 2013***

**SOIL WATER STORAGE AS RELATED TO WATER BALANCES**

REICHARDT Klaus  
*CENA Centro de Energia Nuclear Na Agricultura  
Universidade de Sao Paulo, Av. Centenario 303  
Sao Dimas, CP 96, SP 13400-970 Piracicaba  
BRAZIL*

# SOIL WATER STORAGE AS RELATED TO WATER BALANCES

Klaus Reichardt<sup>1</sup>, Durval Dourado-Neto<sup>2</sup>, Ana Paula Schwantes<sup>2</sup>  
and Luis Carlos Timm<sup>3</sup>

<sup>1</sup>Soil Physics Laboratory, Center for Nuclear Energy in Agriculture (CENA), University of São Paulo (USP), Piracicaba, SP, Brazil. E-mail: klaus@cena.usp.br

<sup>2</sup> Crop Science Department, Superior College of Agriculture “Luiz de Queiroz” (ESALQ), USP, Piracicaba, SP, Brazil.

<sup>3</sup>Department of Rural Engineering, Agronomy College Eliseu Maciel (FAEM), University of Pelotas (UFPel), Pelotas, RS, Brazil.

Soil water storage ( $S$ , mm) is the quantification of the amount of water present in the soil reservoir, at any time  $t$ . Soil water at time  $t$  might be moving in any direction or be at equilibrium. On several instances soil water movement is relatively slow and in such situation we will calculate  $S$ . It is the main component of water balances, that are the contabilization of the in and out water flows of an elemental soil volume (Figure 1).

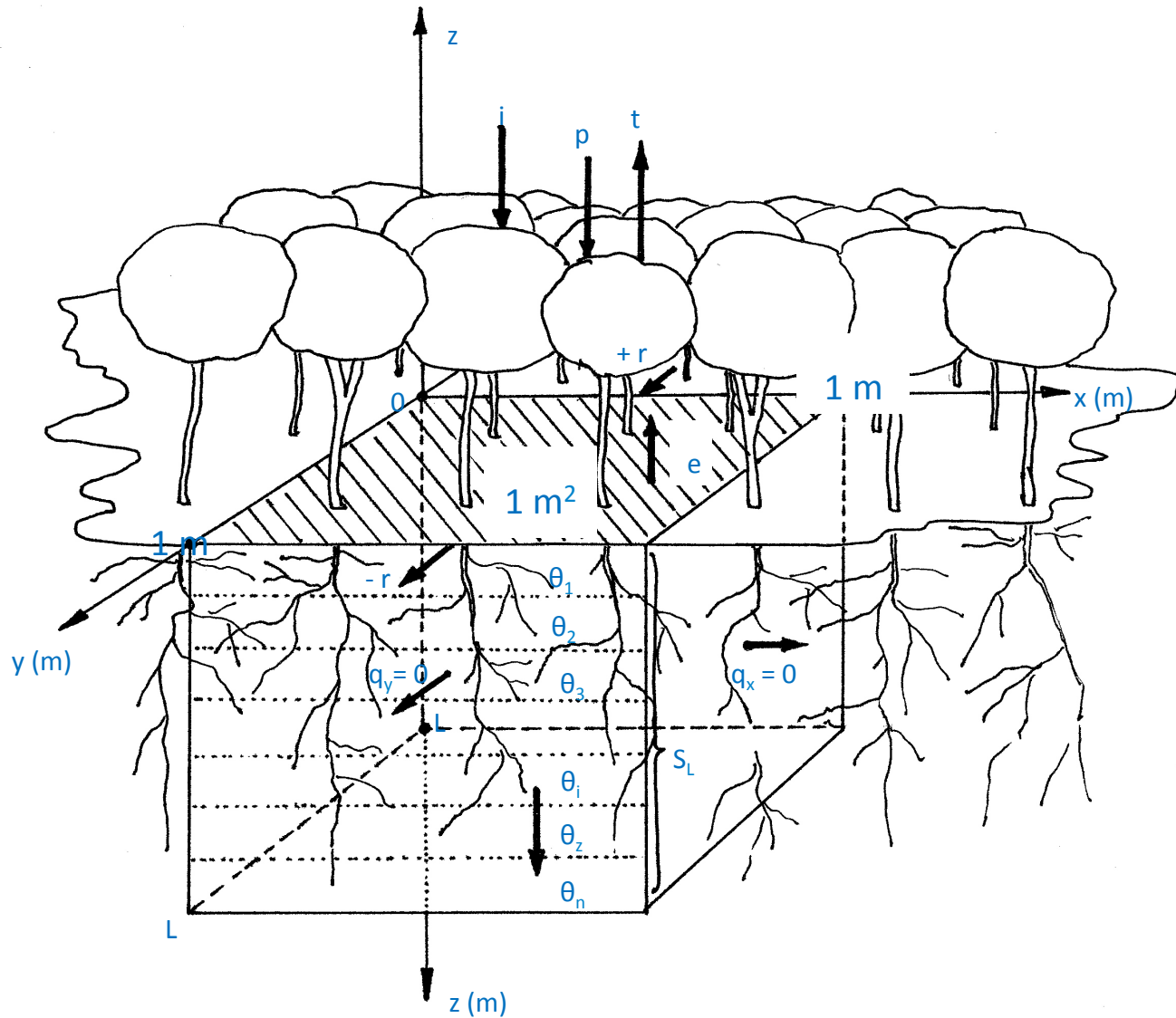


Figure 1. Schematic view of the volume element and of the fluxes that compose the water balance.

$$p + i - et \pm r \pm q_L = \frac{\partial S}{\partial t} \quad (1)$$

$$\int_{t_i}^{t_f} (p + i - et \pm r \pm q_L) dt = \int_{t_i}^{t_f} \int_0^L \frac{\partial \theta}{\partial t} dz dt \quad (2)$$

$$P + I - ETa \pm R \pm Q_L = \Delta S = S(t_f) - S(t_i) \quad (3)$$

$$S = \int_0^L \theta(z) dz \quad (4)$$

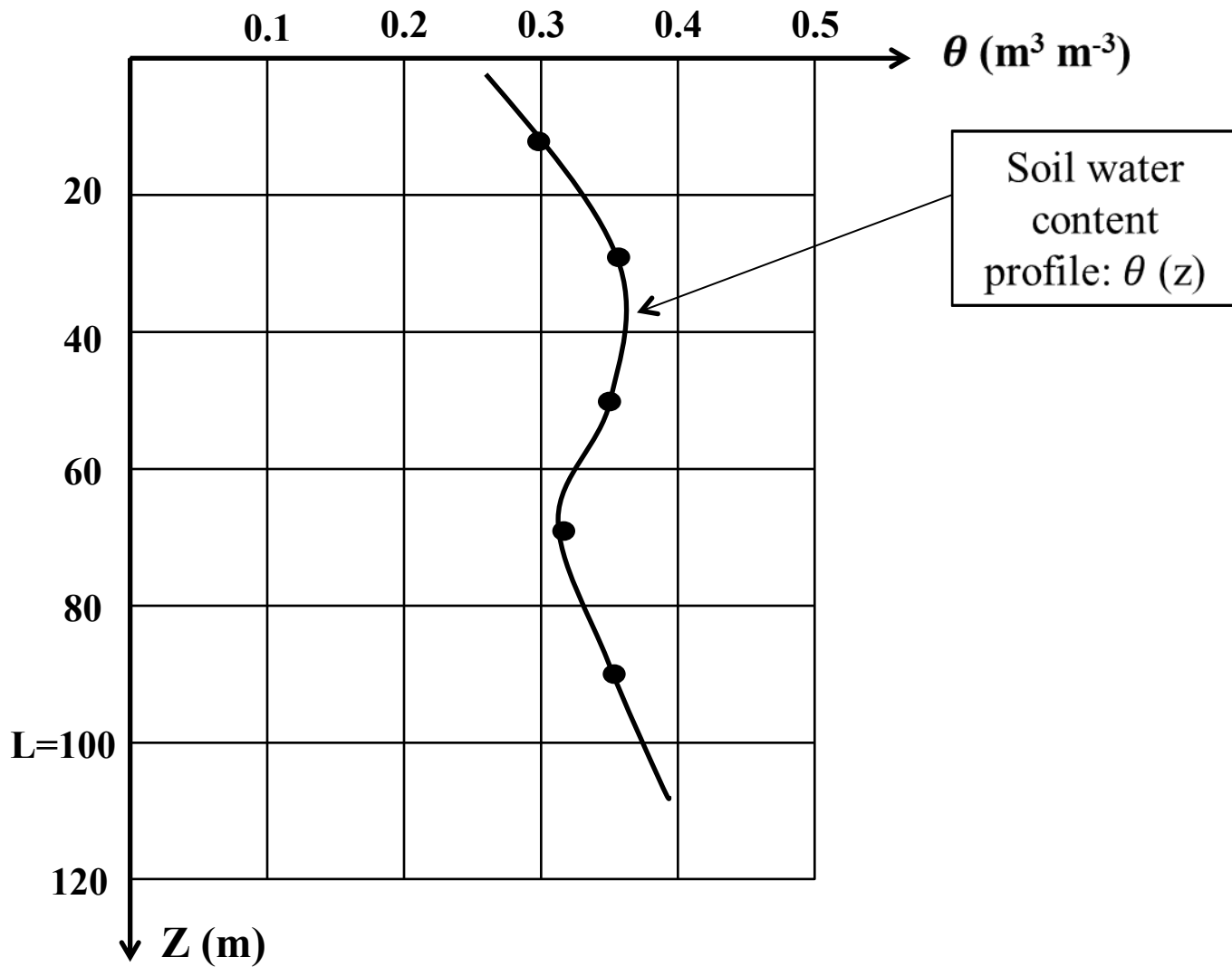


Figure 2. An example of a soil water content profile.

$$\begin{aligned}
S &= \sum_{i=1}^5 \theta_i \Delta_z = \theta_1 \Delta_z + \theta_2 \Delta_z + \dots + \theta_5 \Delta_z \\
&= (\theta_1 + \theta_2 + \dots + \theta_5) \Delta_z \\
&= \left[ \frac{(\theta_1 + \theta_2 + \dots + \theta_5)}{5} \right] = 5 \Delta_z \\
&= \bar{\theta} * L
\end{aligned}$$

Which means that S is equal to the average of  $\theta$  multiplied by the layer L over which the average  $\bar{\theta}$  was taken. Since  $\theta$  is dimensionless, if we express L in mm, S will also be obtained in mm. for the case of Fig. 2, we have:

$$\begin{aligned}
S &= (0.3 + 0.35 + 0.37 + 0.31 + 0.34) 200 \\
&= 0.344 \text{ m}^3 \text{ m}^{-3} \times 1000 \text{ mm} \\
&= 334 \text{ mm}
\end{aligned}$$

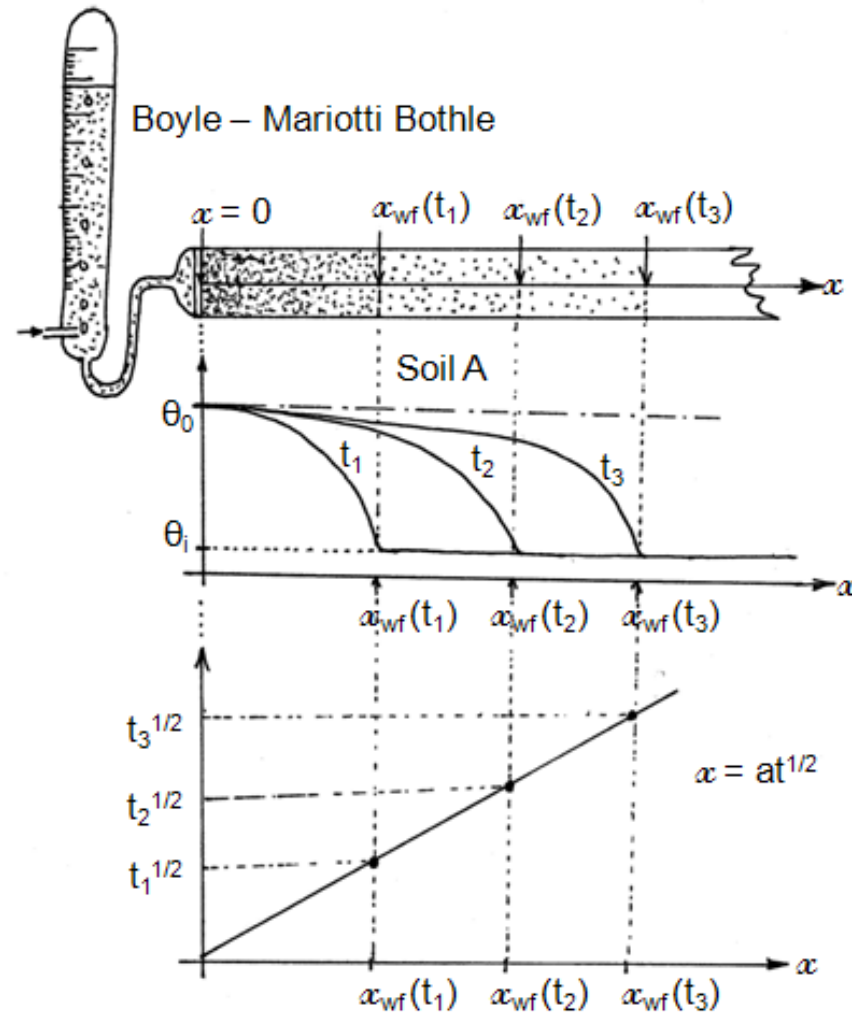


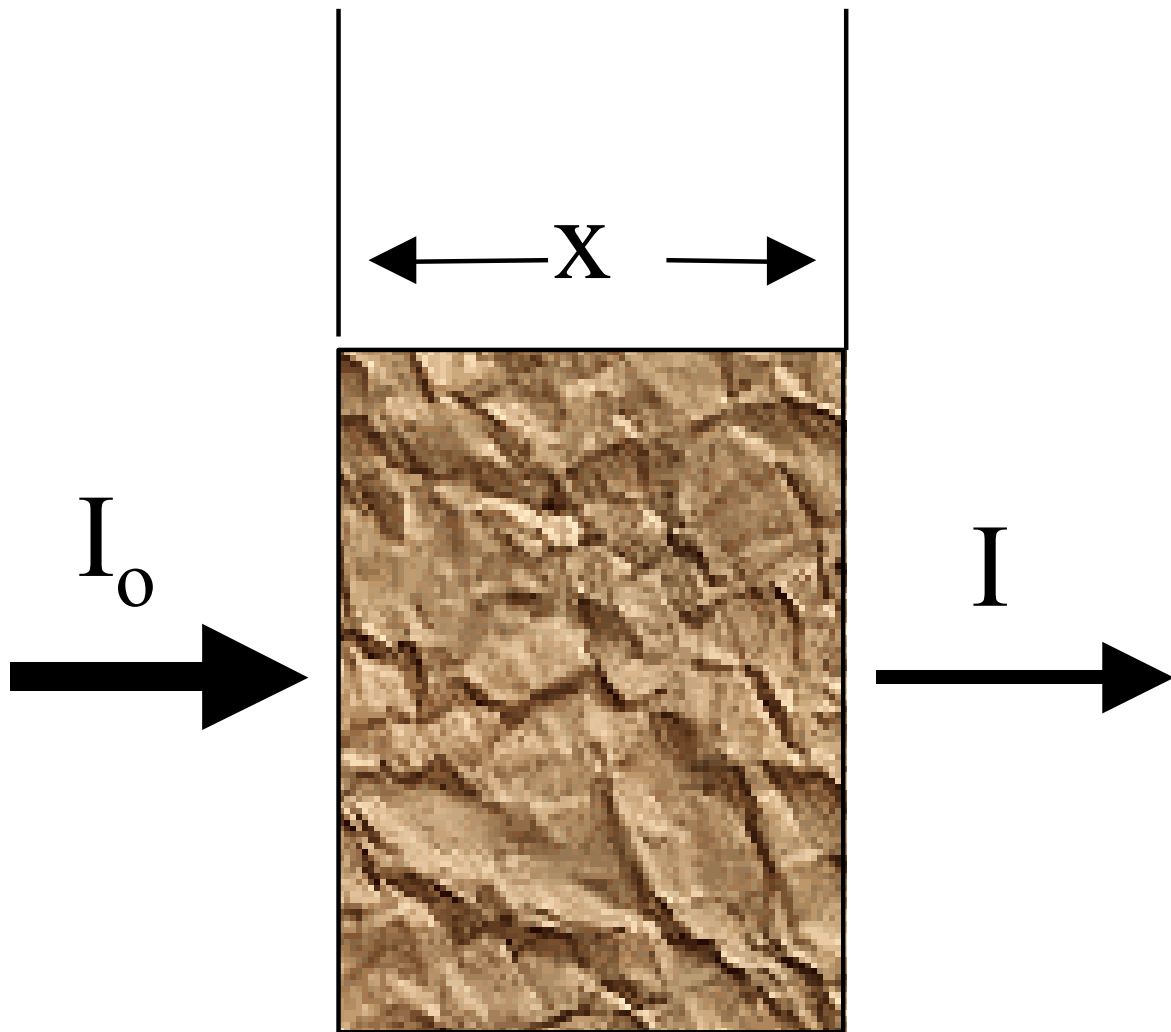
Figure 3. Experimental arrangement to study the horizontal infiltration using transparent acrylic columns for an initially dry soil and the advancement of wetting front as a function of the square root of time.

# ELETROMAGNETIC WAVE ATTENUATION IN SOIL PHYSICS

$$E = hf \quad ; \quad c = \lambda f = \text{constant}$$

h being Plank's constant.

Radiation type	Wave length $\lambda$ ( $\mu\text{m}$ )
Gamma	$4 \times 10^{-8} - 1 \times 10^{-4}$
X	$1 \times 10^{-5} - 0.01$
ultra violet	0.01 – 0.38
visible light	0.38 – 0.78
infrared	0.78 – 1.000



$$I = I_0 e^{-\mu \cdot \rho \cdot x}$$

**High voltage source**

**Amplifier and analyser**

**Counter**

**Collimation wholes**

**Pre-amplifier**

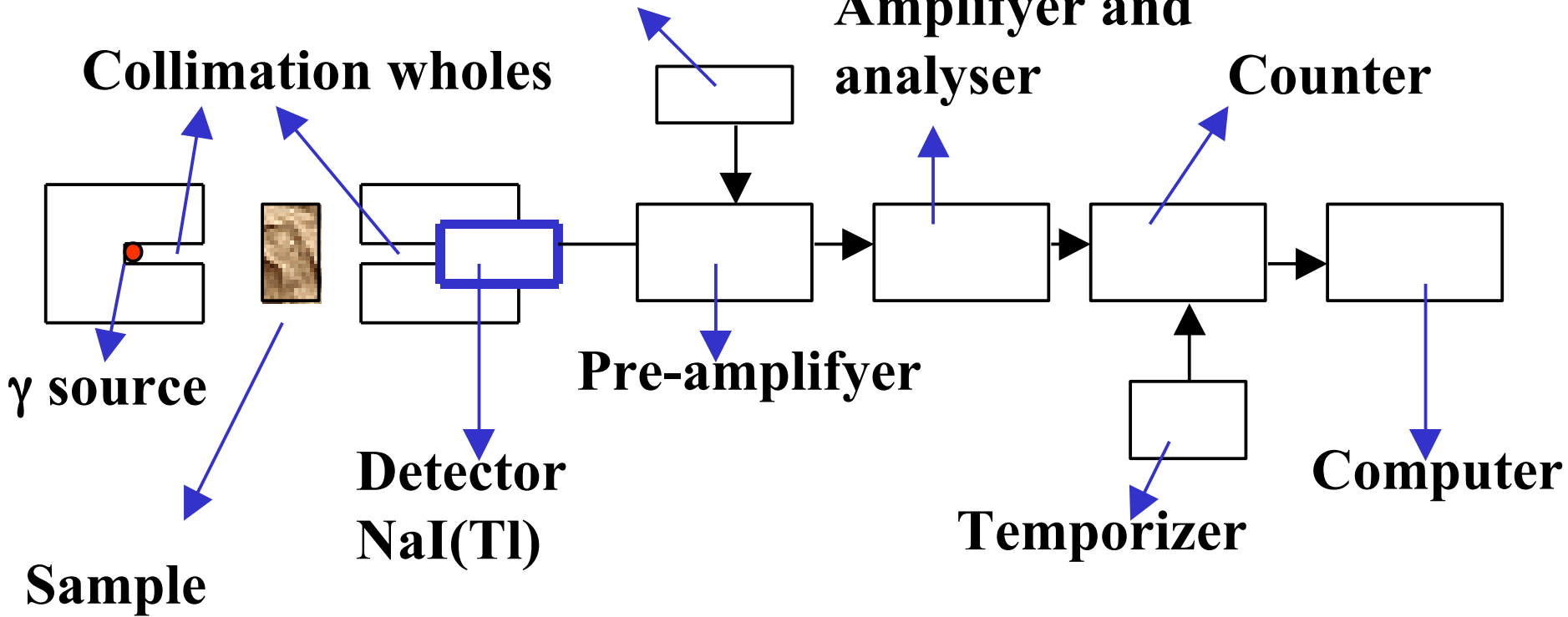
**Temporizer**

**Computer**

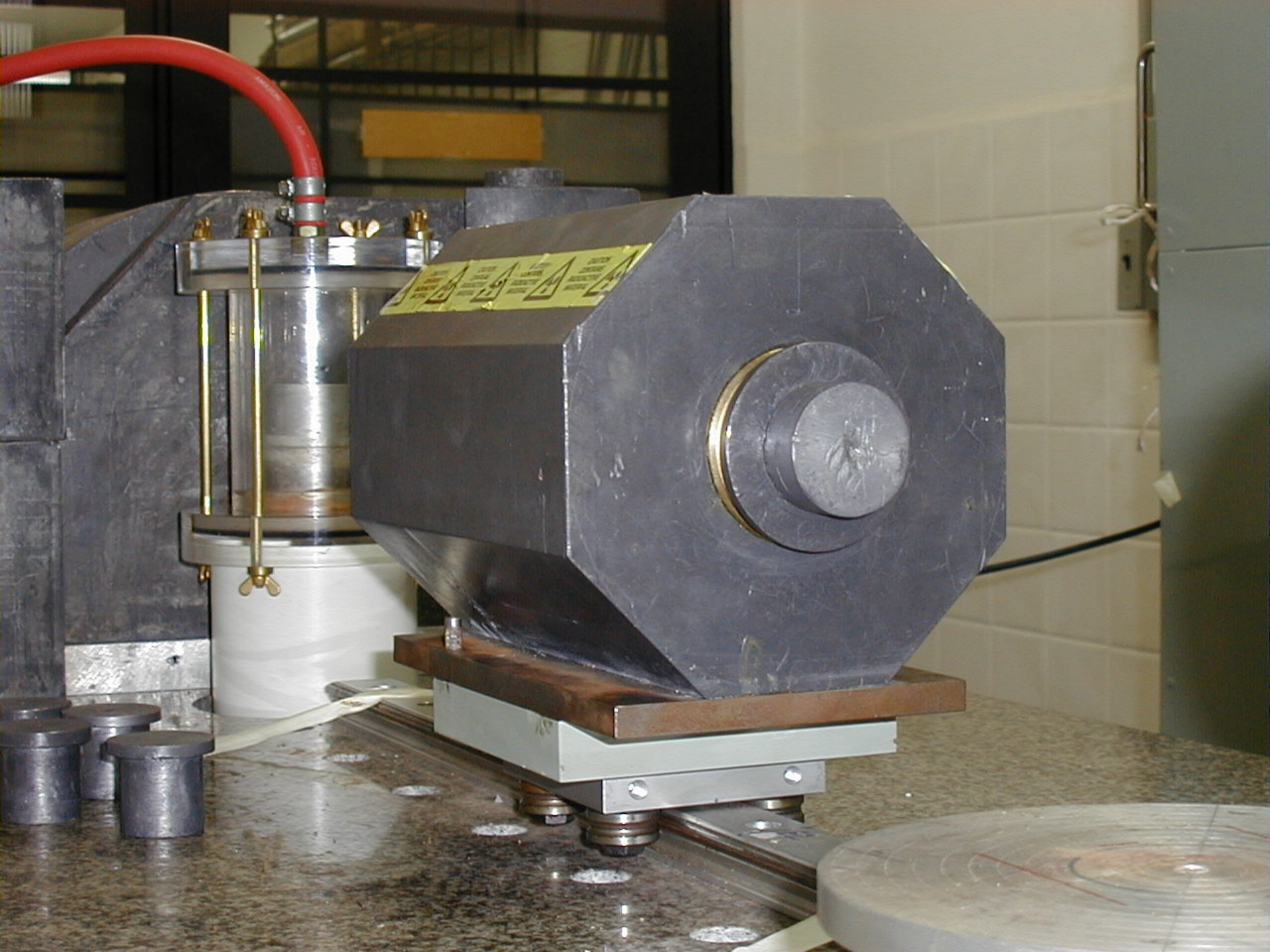
**$\gamma$  source**

**Detector  
NaI(Tl)**

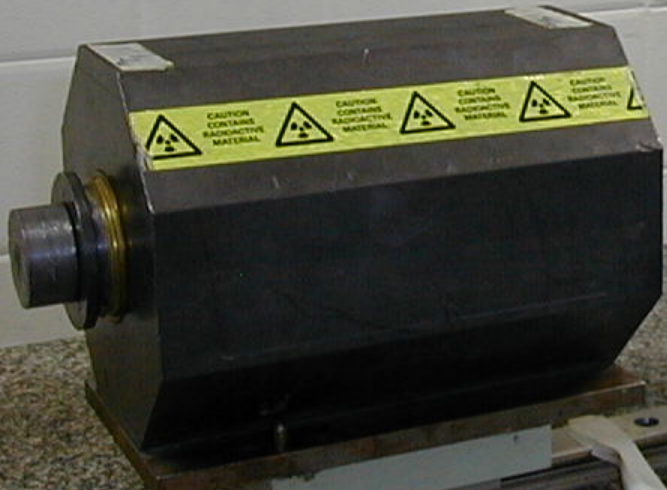
**Sample**







CAUTION  
RADIOACTIVE MATERIAL



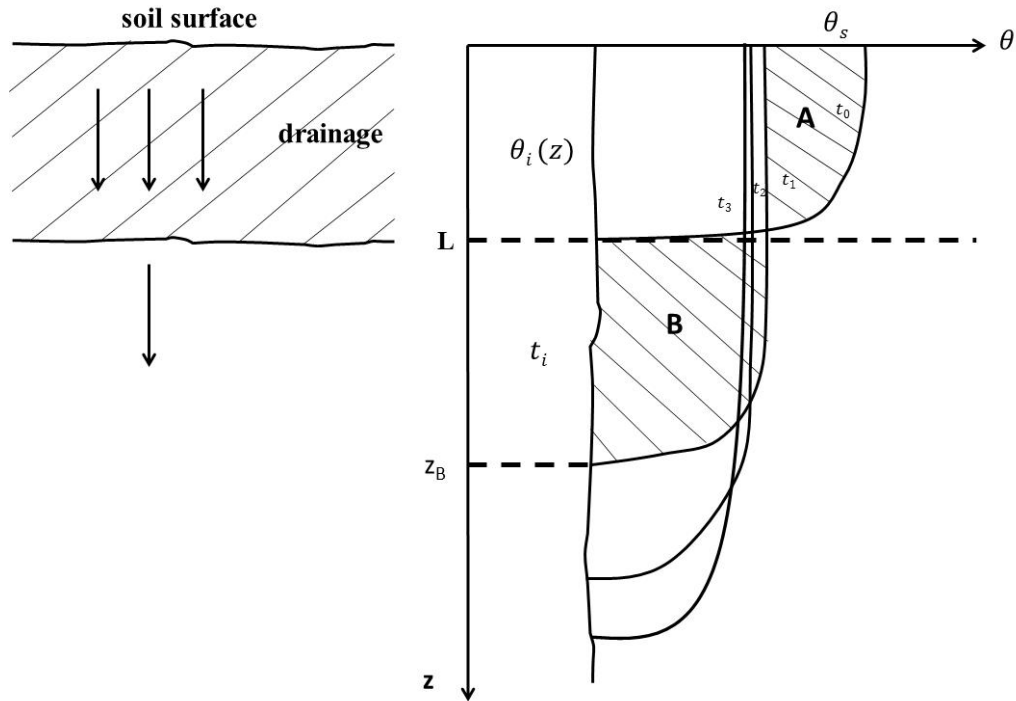
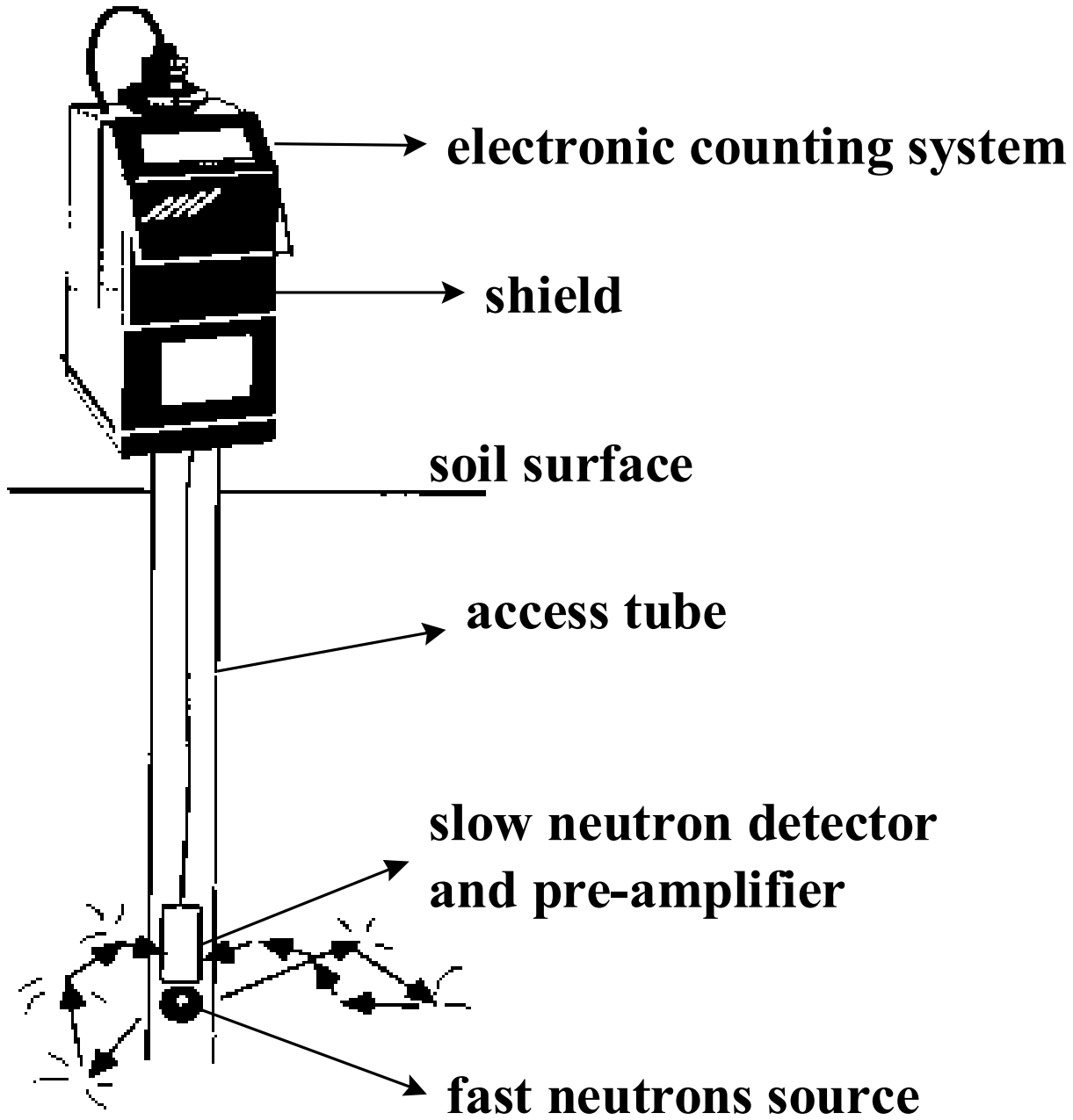


Figure 4. Soil water content profiles during an internal drainage experiment to calculate soil hydraulic conductivity of layer L.

Note that in Fig. 4 the area A represents of the soil layer 0 – L m, between times  $t_0$  and  $t_1$ , which is equivalent to area B (also between times  $t_0$  and  $t_1$ ) because the soil surface was covered with a plastic sheet so that eventual rainfall or irrigation could not contribute to changes in S, and also no evaporation was possible at soil surface:

$$A = \Delta S_L = S_L(t_0) - S_L(t_1) = \int_0^L \theta(t_0) dz - \int_0^L \theta(t_1) dz$$

$$B = \Delta S_{(z_b-L)} = \int_L^{z_b} \theta(t_1) dz - \int_L^{z_b} \theta(t_i) dz$$

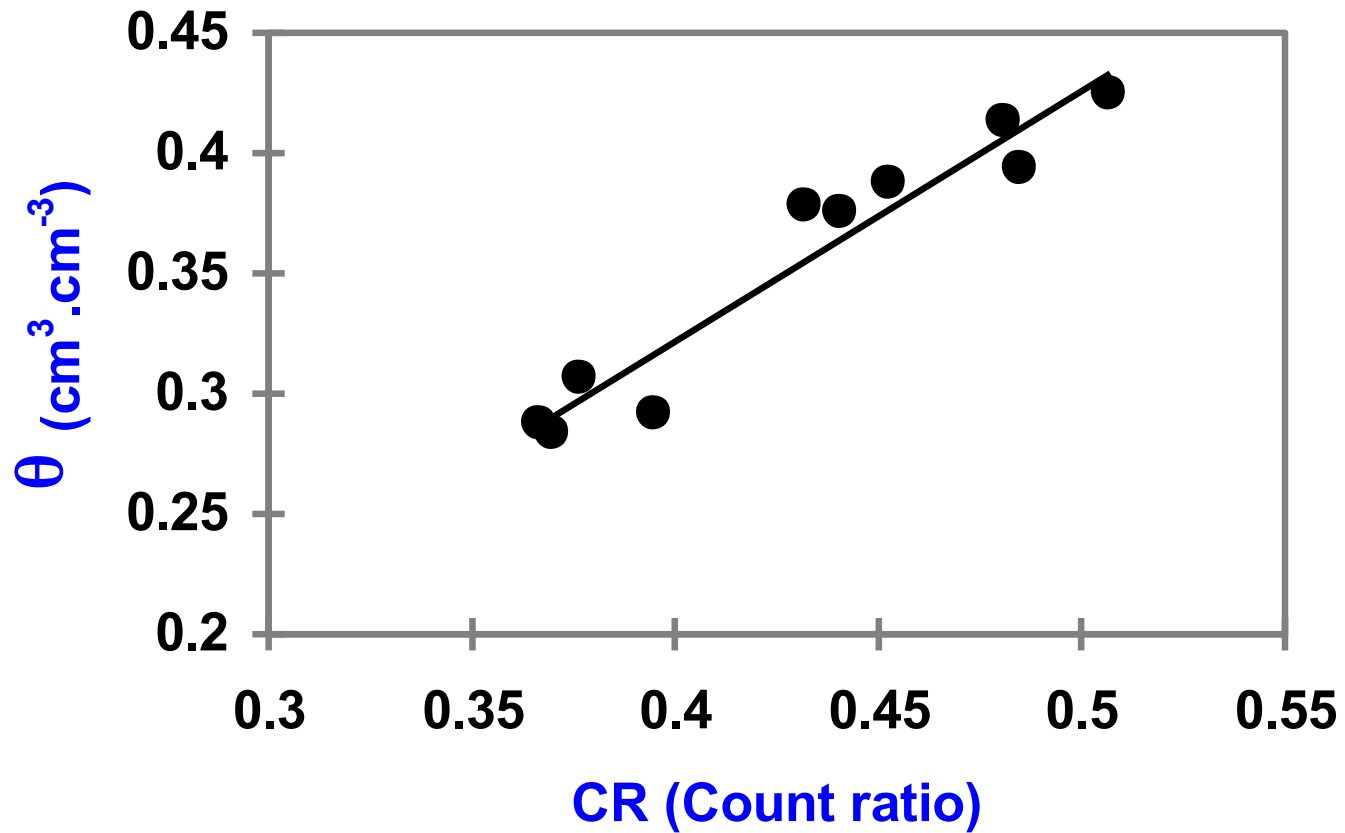






**Table 1**  
**Number of elastic collisions necessary to reduce the energy**  
**of a neutron from 2 MeV to 0.025 eV**

Target Isotope	Number of Collisions
$^1\text{H}$	18
$^2\text{H}$	25
$^4\text{He}$	43
$^7\text{Li}$	68
$^{12}\text{C}$	115
$^{16}\text{O}$	152
$^{238}\text{U}$	2172



Calibration equation obtained with Table 3 data.

**Table 5:** Soil water storage  $S_L(t_i)$ , standard deviations  $s(S_L)$ , and coefficients of variation (CV) of each period analyzed.

Balance	Period	DAB	$S_L$							
			1	2	3	4	5	$\overline{S_L}$	$s(S_L)$	CV
1	01/09 to 15/09	0_14	250.2	260.8	203.4	254.6	257.2	245.2	23.7	9.7
2	15/09 to 29/09	14_28	261.0	271.1	221.0	265.6	268.3	257.4	20.7	8.0
3	29/09 to 13/10	28_42	255.9	265.6	213.1	259.3	262.4	251.3	21.6	8.6
4	13/10 to 27/10	42_56	272.3	284.5	242.8	303.0	286.9	277.9	22.5	8.1
5	27/10 to 10/11	56_70	269.9	280.3	232.8	292.2	279.9	271.0	22.8	8.4
6	10/11 to 24/11	70_84	263.2	276.0	221.5	278.7	276.8	263.3	24.1	9.2
7	24/11 to 08/12	84_98	273.0	287.4	238.7	296.3	282.5	275.6	22.3	8.1
8	08/12 to 22/12	98_112	286.3	306.7	262.3	317.2	293.1	293.1	21.0	7.2
9	22/12 to 05/01	112_126	277.9	299.8	249.8	309.2	288.0	284.9	22.9	8.0
10	05/01 to 19/01	126_140	288.3	312.9	271.4	336.9	299.9	301.9	24.8	8.2
11	19/01 to 02/02	140_154	288.0	311.4	270.2	328.0	303.2	300.2	22.1	7.4
12	02/02 to 16/02	154_168	380.0	380.2	324.5	384.3	380.6	369.9	25.5	6.9
13	16/02 to 01/03	168_182	352.1	354.8	302.6	359.5	350.8	344.0	23.3	6.8
14	01/03 to 15/03	182_196	375.4	382.3	317.4	375.2	375.3	365.1	26.9	7.4
15	15/03 to 29/03	196_210	356.2	364.1	305.4	359.2	357.7	348.5	24.3	7.0
16	29/03 to 12/04	210_224	310.5	314.4	258.0	311.5	306.0	300.1	23.7	7.9
17	12/04 to 26/04	224_238	304.5	317.2	261.9	315.4	305.2	300.8	22.5	7.5
18	26/04 to 10/05	238_252	305.0	313.3	261.0	318.2	309.2	301.3	23.1	7.7
19	10/05 to 24/05	252_266	301.0	306.4	253.0	308.7	305.4	294.9	23.6	8.0
20	24/05 to 07/06	266_280	300.2	304.8	254.3	306.1	308.8	294.8	22.9	7.8
21	07/06 to 21/06	280_294	360.1	359.9	312.8	356.2	354.3	348.7	20.2	5.8
22	21/06 to 05/07	294_308	348.4	348.7	293.3	342.0	348.7	336.2	24.2	7.2
23	05/07 to 19/07	308_322	327.7	327.7	274.8	321.6	329.2	316.2	23.3	7.4
24	19/07 to 02/08	322_336	350.7	345.4	306.0	353.7	355.3	342.2	20.6	6.0
25	02/08 to 16/08	336_350	341.4	334.6	290.7	337.9	341.7	329.3	21.7	6.6
26	16/08 to 30/08	350_364	334.1	324.3	280.4	322.9	327.4	317.8	21.4	6.7

# SOIL WATER STORAGE CHANGES MEASURED IN A SOYBEAN CROP IN PIRACICABA, BRAZIL

A soybean (*Glycine max* (L.) Merrill) crop was established on a Oxisol in Piracicaba, Brazil, and for management purposes the soil water storage  $S$  was monitored during the whole cycle. The novelty of the experiment was the continuous measurement of the soil water matric potential  $h$  (m) using polymer tensiometers. Readings of  $h$  were then transformed into  $\Theta$  through the use of a soil water retention curve, to further calculate water storages.

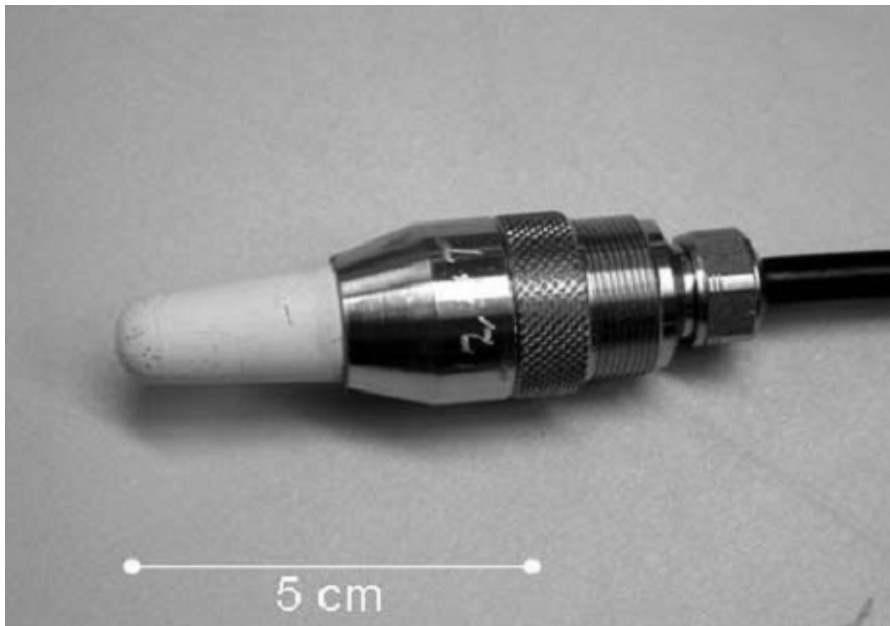


Figure 1 – Polymer tensiometer. Source: Durigon; de Jong Van Lier (2011).

Figure 1a – Details of the polymer tensiometer showing the ceramic disc of  $\alpha$ -Al<sub>2</sub>O<sub>3</sub> (1), a membrane of  $\gamma$ -Al<sub>2</sub>O<sub>3</sub> (2), inox steel capsule (3), polymer chamber (4), pressure transducer (5), and a synthetic ring (6). Source: Bakker et al. (2007).

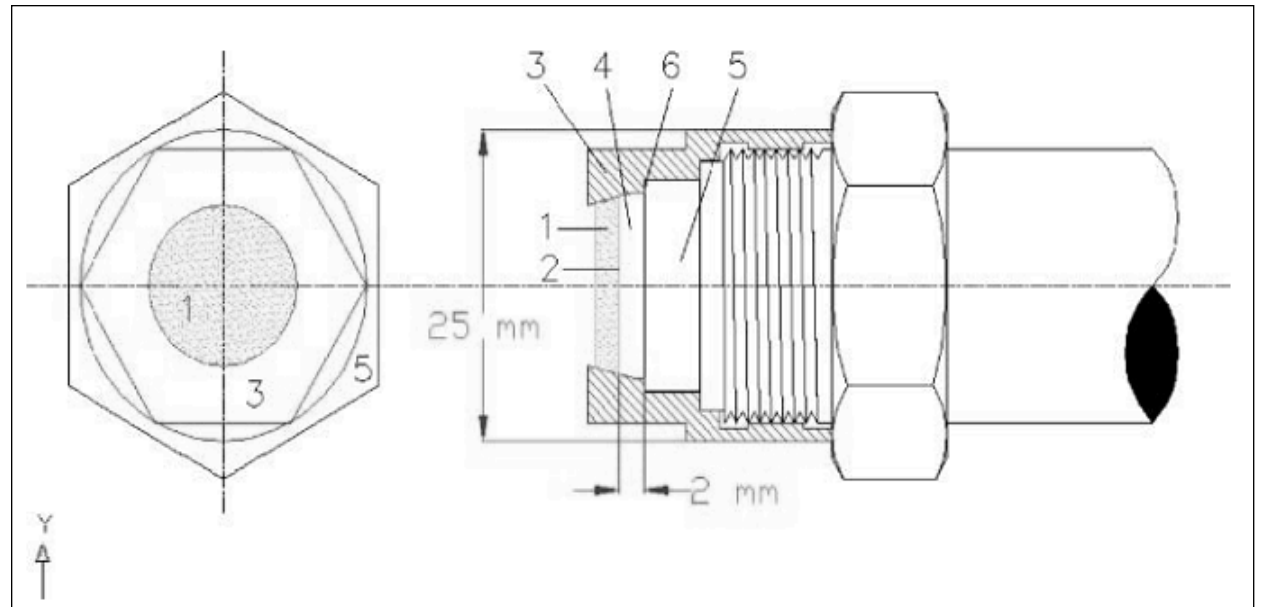




Figure 2. View of the soybean crop at initial growth stage. Piracicaba, 2012.

$$\theta = \theta_r + \frac{(\theta_s - \theta_r)}{[1 + (\alpha h)^n]^m}$$

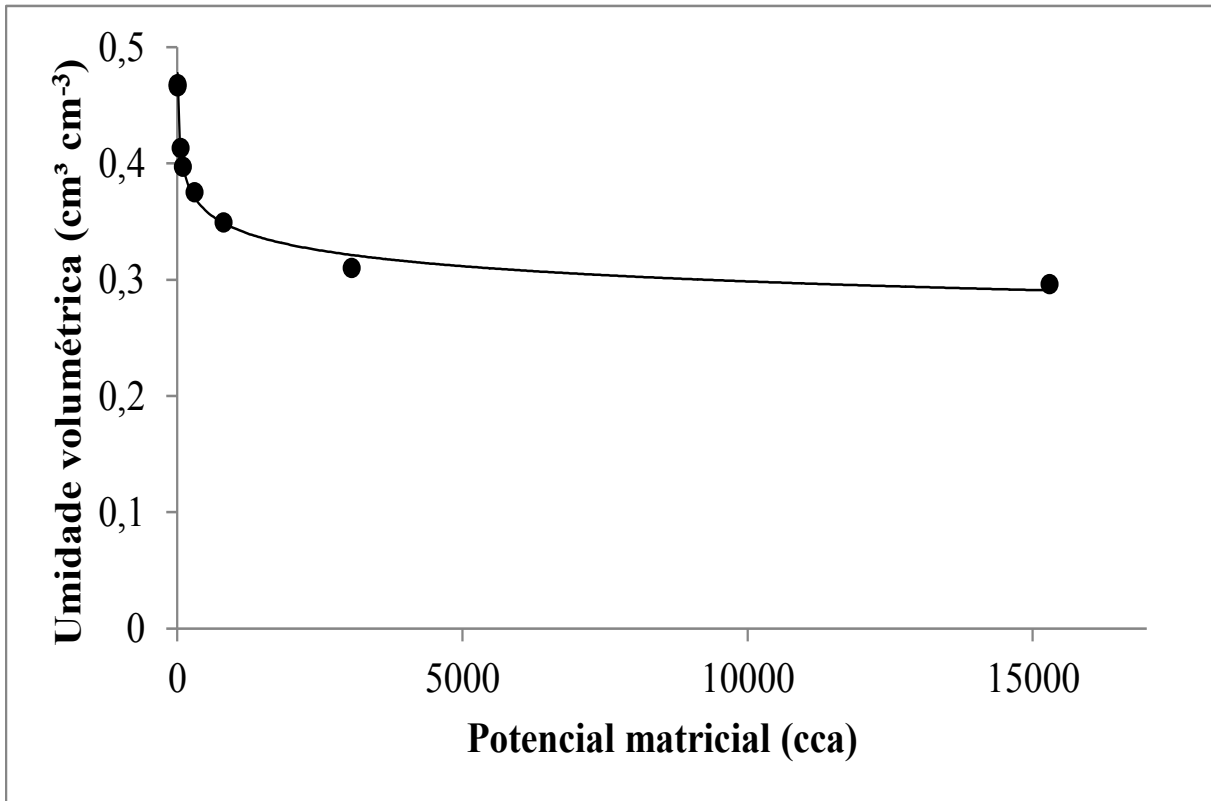


Figure 5 – Average soil water retention curve obtained with 250 points. Source: Moraes (1991).

Another way to look at soil water storage, is using the available water (AW) concept. This concept assumes that the available water to plants lies between a maximum  $\theta$  value, called  $\theta_{FC}$  fc, and a minimum  $\theta_{PWP}$ . The water between  $\theta_s$  and  $\theta_{FC}$  is considered to be subject to gravitational drainage, not being available to plants. The water below  $\theta_{PWP}$  is considered to be at such low matric potentials the plants cannot make use of it. With these concepts, we can define the water holding capacity of a soil (AWC) as  $[\theta_{FC} - \theta_{PWP}]$ , and soil water storages  $S$  can also be defined as:

$$S = (\bar{\theta} - \theta_{PWP}) * Z_e \quad (2)$$

Where  $Z_e$  is the rooting depth, considered in this soybean experiment as 0.4 m or 400 mm. Equation (4) was applied layer per layer to obtain the final value of  $S$ .

During the cropping cycle the crop receives water from rainfall  $P$  or irrigation  $I$ , and every time the soil reaches the AWC, the excess of water is drained below root zone or is lost at the surface as runoff. Within the AWC range, water is either evaporated at the soil surface or transpired by plants, resulting the evapotranspiration  $ET$ . Water is not equally available in the whole range of the AWC, water extraction becomes more and more difficult as the PWP is reached. This is due to drastic decreases in soil hydraulic conductivity as the soil dries out.

There are several models that try to describe the process of water extraction from the soil by plants, and in the previous lecture we mentioned three commonly used models: Thornthwaite & Mather; Rijtema & Aboukhaled; and Dourado & van Lier. For the first, the decrease in S follows the model:

$$S_i = AWC e^{-\frac{\theta}{(\theta_{FC} - \theta_{PWP})}} \quad (3)$$

Rijtema and Aboukhaled (1975) take into consideration a water availability factor  $p$  for the estimation of S, which decreases as:

$$S_i = (1 - p)AWC \exp\left(\frac{p - \frac{\theta}{(\theta_{FC} - \theta_{PWP})}}{(1-p)}\right) \quad (4)$$

Dourado and van Lier (1993) assume a cossenoidal rate of ET decrease, and S decreases as:

$$S_i = (1 - p)AWC \left\{ 1 - \frac{2}{\pi} \arctg \left[ \frac{\pi}{2} \left( \frac{\left( \frac{\theta}{(\theta_{FC} - \theta_{PWP})} \right)^{-p}}{1-p} \right) \right] \right\} \quad (5)$$

Crop yield is severely reduced by water shortage. Therefore, the concept of water depleted yield  $Y_r$  was defined by Doorenbos e Kassam (1994):

$$Y_r = \left[ 1 - ky \left( 1 - \frac{ET_r}{ETC} \right) \right] * Y_o \quad (6)$$

$ky$  being a crop water stress sensitivity factor, that changes as the crop develops;  $ET_r$  the actual evapotranspiration; and  $ETC$  the maximum evapotranspiration of the crop, and:

$$Y_o = Fb * C_{IAF} * C_{RESP} * C_{COL} * C_U * NDC \quad (7)$$

$Fb$  is the Gross photosynthesis;  $C_{IAF}$  a correction factor related to growth phase and leaf area;  $C_{RESP}$  a correction factor related to plant respiration;  $C_{COL}$  a correction for the harvest index;  $C_U$  a correction the water content of the harvested matter, and  $NDC$  the length of the growth period, all proposed by Pereira; Angelocci; Sentelhas (2002).

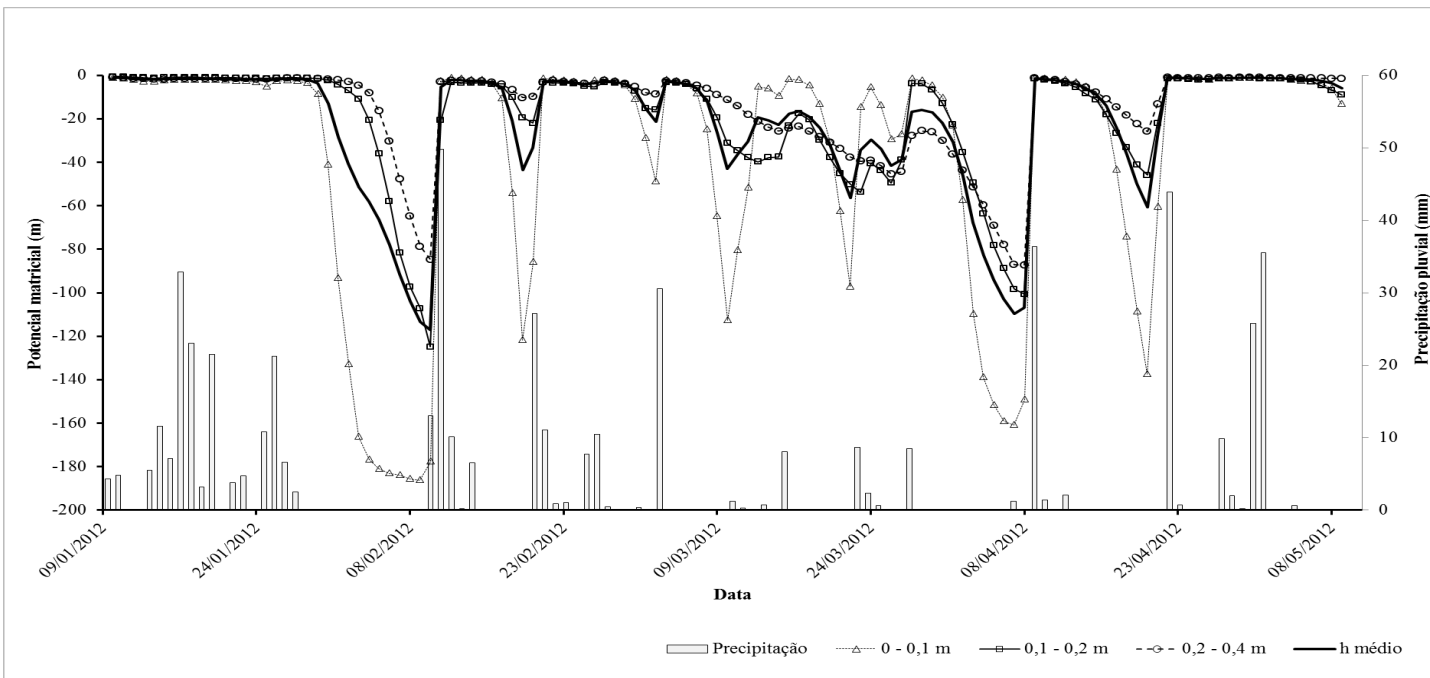


Figure 7. Matric potential  $h$  (m) measured by polymer tensiometers and rainfall (mm).

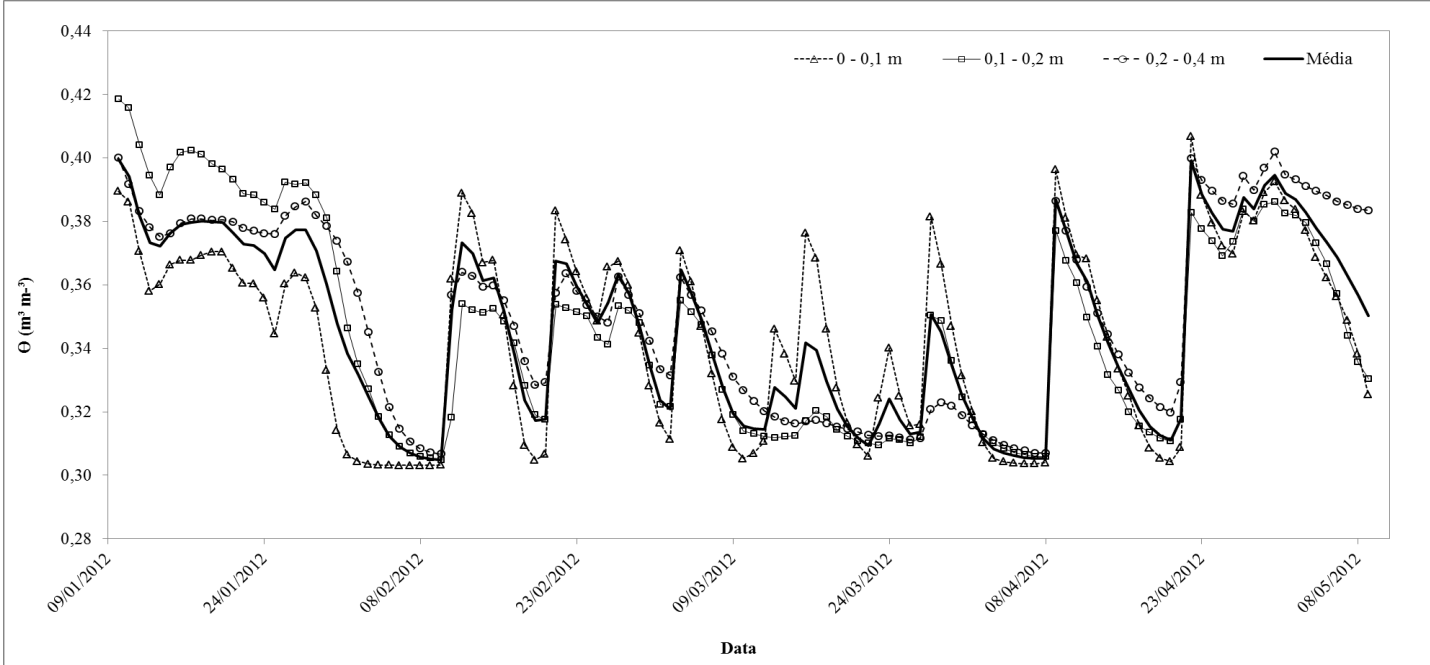


Figure 8. Soil water content for the layers 0-0.1 m; 0.1-0.2 m and 0.2-0.4 m and their average.

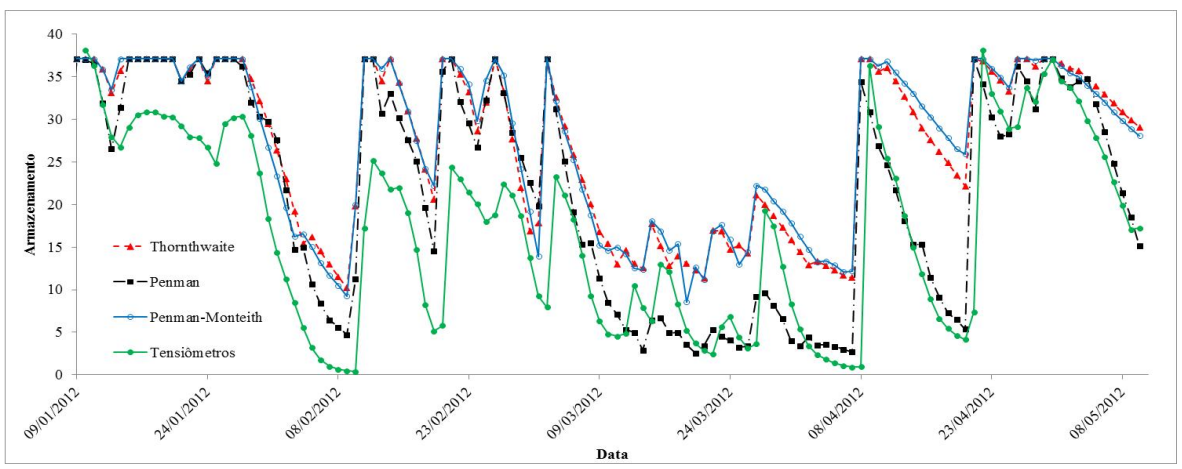


Figura 9 - Armazenamento de água (mm) medido pelos tensiômetros e estimado pelo método de **Thornthwaite e Mather** com a evapotranspiração de cultura estimada pelos métodos de Thornthwaite, Penman e Penman e Monteith

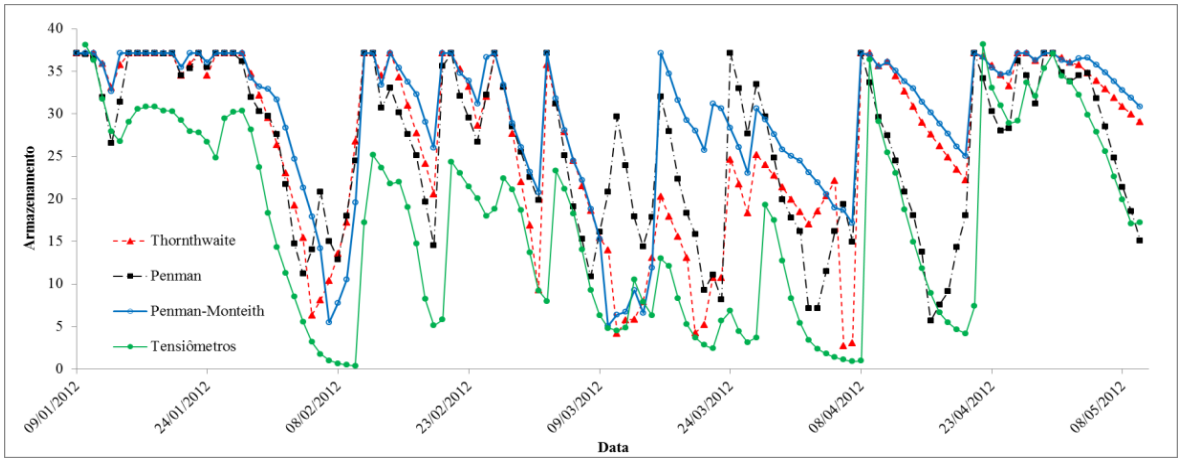


Figura 10 - Armazenamento de água (mm) medido pelos tensiômetros e estimado pelo método de **Rijtema e Aboukhaled** com a evapotranspiração de cultura estimada pelos métodos de Thornthwaite, Penman e Penman e Monteith

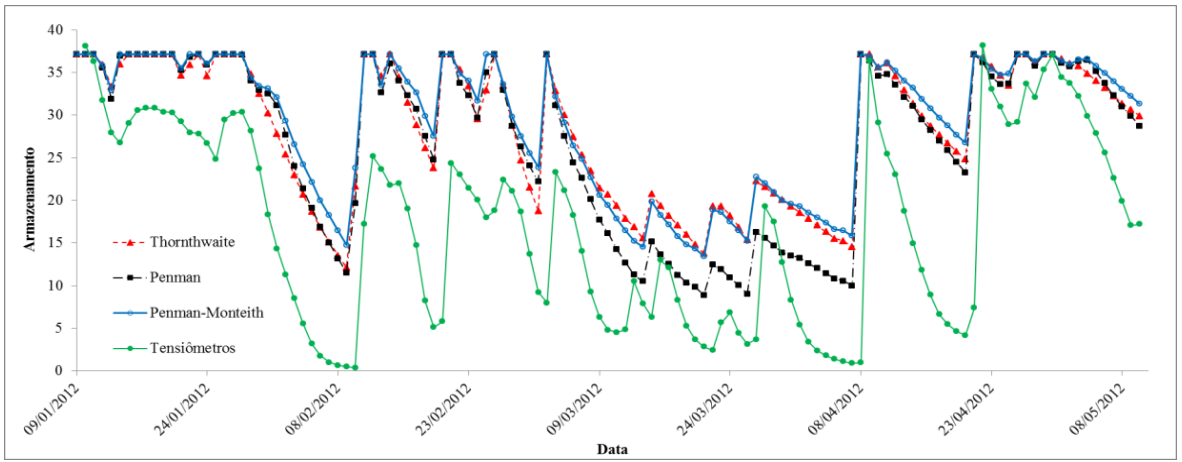


Figura 11 - Armazenamento de água (mm) medido pelos tensiômetros e estimado pelo método **Cossenoidal** com a evapotranspiração de cultura estimada pelos métodos de Thornthwaite, Penman e Penman e Monteith

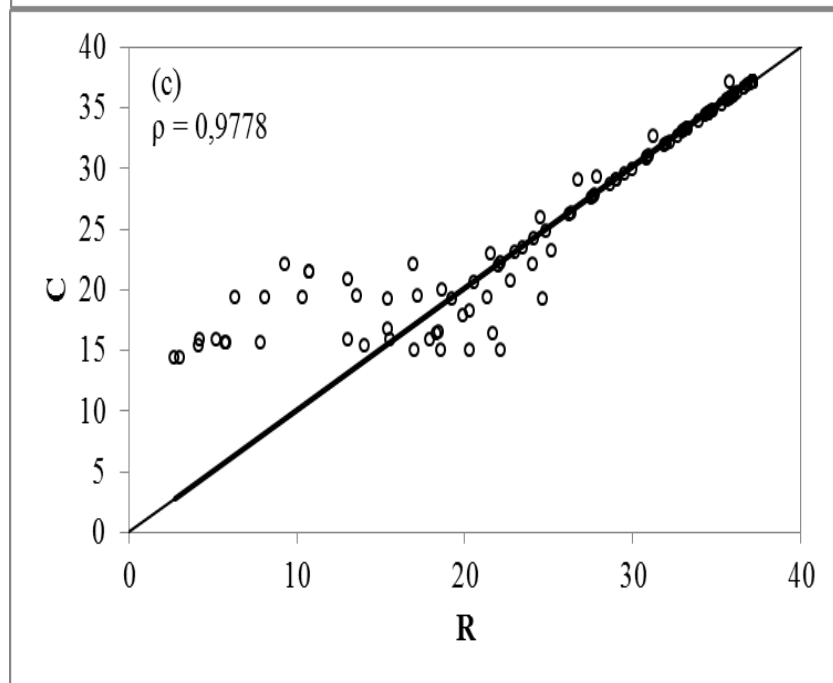
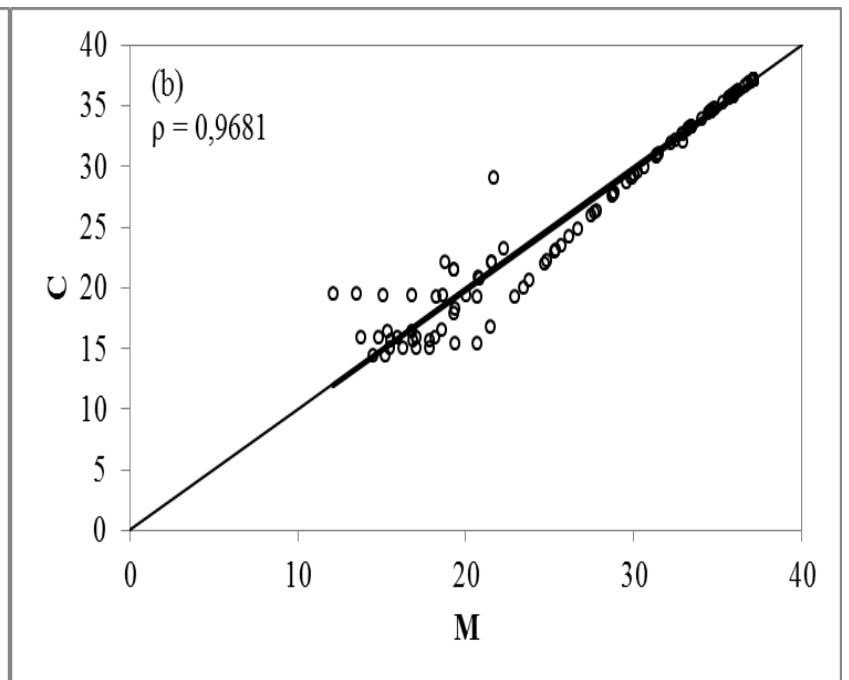
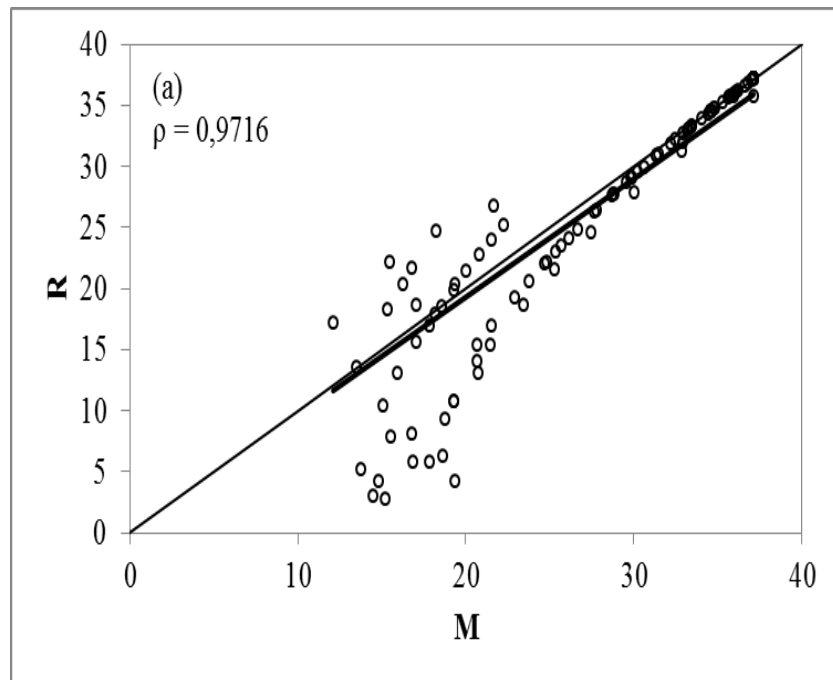


Figura 12 - Análise de regressão entre os armazenamentos de água estimados pelos métodos de balanço hídrico de: (a) Thornthwaite e Mather (M) e Rijtema e Aboukhaled (R); (b) Thornthwaite e Mather (M) e Cossenoidal (C); e (c) Rijtema e Aboukhaled (R) e Cossenoidal (C), com estimativa da ETC pelo método de **Thornthwaite**

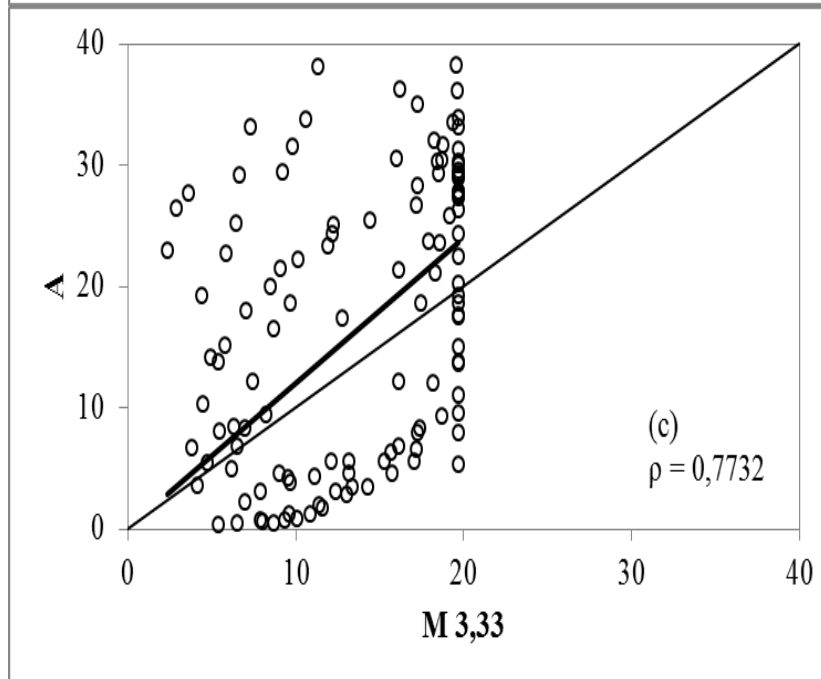
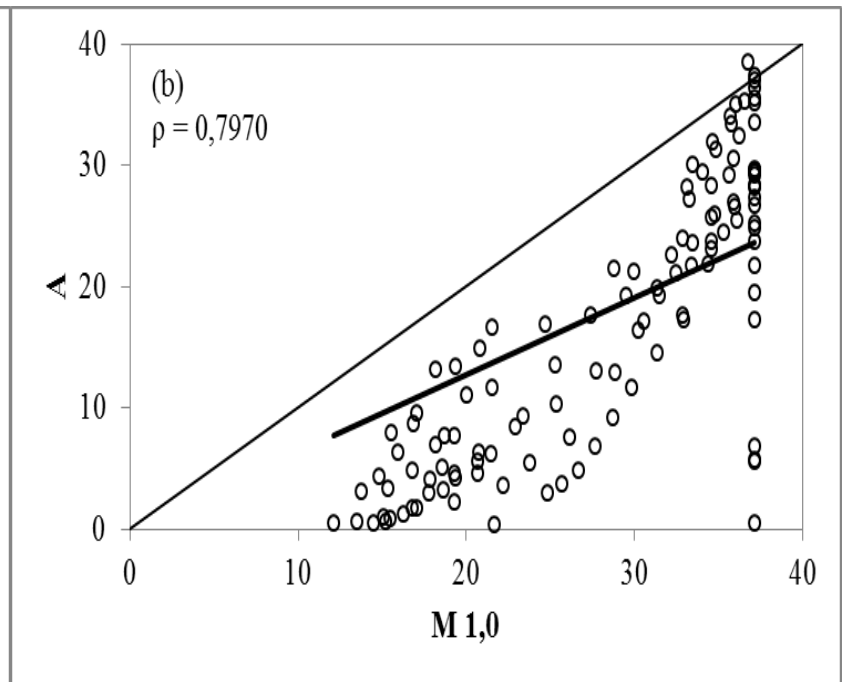
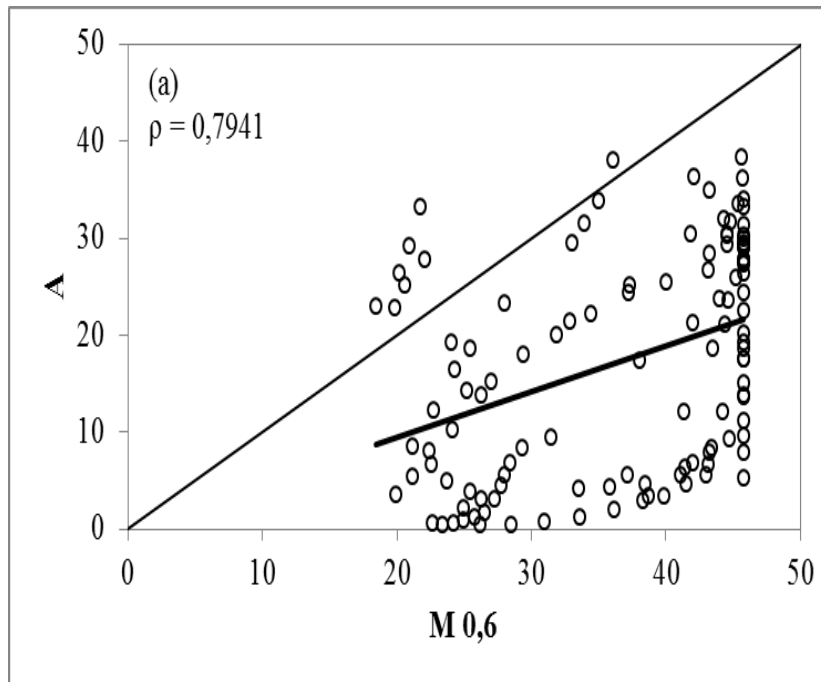


Figura 18 - Análise de regressão entre o armazenamento de água medido pelos tensiômetros de polímero (A) com o armazenamento de água estimado pelo métodos de balanço hídrico de Thornthwaite e Mather (M) com a CAD de 45,8 mm (0,6 m H<sub>2</sub>O, a); de 37,1 mm (1,0 m H<sub>2</sub>O, b); e de 19,7 mm (3,33 m H<sub>2</sub>O, c)

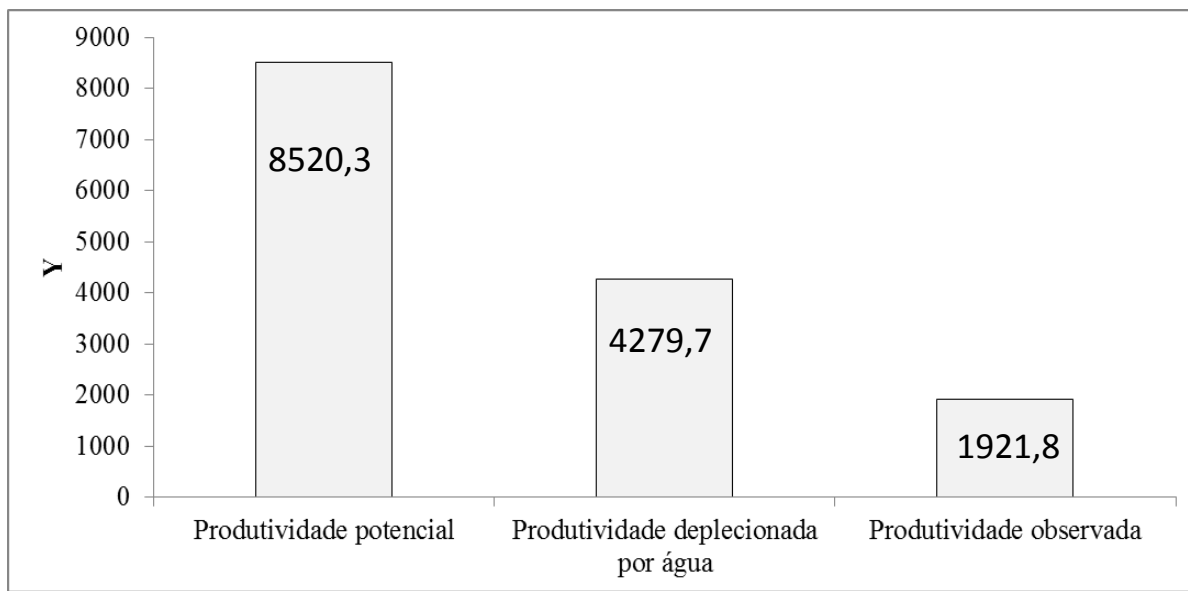


Figura 19 - Produtividade potencial ( $Y_o$ , kg ha<sup>-1</sup>), produtividade deplecionada por água ( $Y_r$ , kg ha<sup>-1</sup>) e produtividade observada ( $Y_c$ , kg ha<sup>-1</sup>)